Desalination and Water Treatment
www.deswater.com
doi: 10.5004/dwt.2021.26562

210 (2021) 365–376
January

Expeditious and enhanced sequestration of heavy metal ions from aqueous environment by papaya peel carbon: a green and low-cost adsorbent

Jyoti Mittal[a], Rais Ahmad[b], Asna Mariyam[a], V.K. Gupta[c], Alok Mittal[a,*]

[a]*Department of Chemistry, Maulana Azad, National Institute of Technology, Bhopal 462003, India, email: aljymittal@gmail.com (A. Mittal), Tel. +91-9893251369; emails: jyalmittal@yahoo.co.in (J. Mittal), asna.maryam1995@gmail.com (A. Mariyam)*
[b]*Environmental Research Laboratory, Department of Applied Chemistry, Aligarh Muslim University, Aligarh 202002, India, Tel. +91-0571-2700920-23 Ext: 3000; Fax: +91-0571-2400528; email: rais45@rediffmal.com*
[c]*King Abdulaziz University, Jeddha, Saudi Arabia, vinodfcy@gmail.com*

Received 17 August 2020; Accepted 11 September 2020

ABSTRACT

In this study, papaya peel carbon (PPC) has been explored as a potential adsorbent for the removal of Pb(II), Cu(II) and Ni(II) from their aqueous phases. Optimum adsorption conditions such as contact time, pH, initial metal ion concentrations, adsorbent dosage and temperature were determined. Optimum pH for the removal of Pb(II) and Ni(II) was found to be 6, while for Cu(II) it was 5. Maximum monolayer adsorption capacity (q_m) was found to be 40.98, 38.02 and 32.25 mg g^{-1} for Pb(II), Cu(II) and Ni(II) ions, respectively. To study the kinetic parameters and mechanism of adsorption process, pseudo-first-order, pseudo-second-order, intraparticle diffusion and Elovich kinetic models were elucidated. D-R adsorption isotherm model best described adsorption of Pb(II) and Ni(II) ions onto PPC, whereas Freundlich adsorption isotherm described adsorption of Cu(II). To further predict the nature of adsorption, thermodynamic parameters such as $\Delta G°$, $\Delta H°$ and $\Delta S°$ were calculated and positive values of $\Delta H°$ indicated endothermic nature of the process. Thus overall results confirmed that PPC can be effectively used as an alternative and low-cost adsorbent for the removal of heavy metal ions Pb(II), Cu(II) and Ni(II).

Keywords: PPC; Adsorbent; Isotherm; Kinetics; Thermodynamics

1. Introduction

Water contamination by heavy metals is an important issue in environmental remediation and separation science due to their non-degradable nature. Due to biomagnification they have the tendency to enter into the food chains, causing severe health problems in human beings and animals [1,2]. Lead metal ions enter into water sources from industries, such as metal plating, lead acid storage battery, pigments, painting, pesticides, smelting, galvanizing, agriculture and mining. Lead can cause severe damage to kidney, brain, reproductive system and nervous system. According to World Health Organization, permissible limit of Pb(II) in drinking water is only 0.01 mg L^{-1} [3,4]. Copper plays an important role in the fundamental and physiological process of organisms. Excessive intake of Cu(II) causes increased blood pressure and respiratory rates, kidney and liver damage, imbalance in cellular processes and damage to the central nervous system. The permissible limit of Cu(II) in drinking water is 0.05 mg L^{-1} [5]. Nickel in aqueous media poses threat to living beings owing

* Corresponding author.

to its acute carcinogenic and neurotoxic effects. According to WHO guidelines, a permissible limit of Ni(II) in aqueous solution is only 0.02 mg L^{-1} [6]. The permissible limits of these metal ions clearly indicate that their eradication from wastewaters is extremely important and suitable physicochemical methods should be adopted for this purpose.

Out of several available physicochemical methods, chemical precipitation/coagulation, membrane technology, electrolytic reduction, ion exchange and adsorption are popular for the removal of heavy metal ions from wastewater [7,8]. The process of adsorption involves separation of an adsorbate from one phase accompanied by its accumulation or concentration at the surface of adsorbent. Adsorption technique has been rapidly gaining importance as wastewater treatment process to treat effluents. The adsorption process has been found to be more advantageous for water pollution control as it needs less investment in terms of both initial cost and land. Second, the treatment equipments are simple in design and easy to operate. The adsorption process imparts no side effect or toxicity to the water and this accounts for the superior removal of inorganic waste constituents as compared with the conventional treatments. The adsorption process provides an attractive alternative treatment, especially if the adsorbent is inexpensive and readily available. Adsorption process is capable of removing the pollutant in its ionic or molecular form without breaking or converting into another product/by-product, therefore it is considered environmentally safe [9]. It is an established fact that the economics and efficacy of adsorption process depends upon quality of adsorbent. As far as removal of heavy metal ions from wastewater is concerned various adsorbent materials have been so far employed; however the search for a cheaper, robust and efficient adsorbent is still going on [10–19].

A low-cost adsorbent is the one that is abundant in nature, a by-product or waste material from another industry or agricultural products and needs very less processing before use. Papaya (*Carica papaya* L.) is a herbaceous plant commonly found in sub-humid tropical regions of Asia, Africa, South America and Central America. India is one of the countries where this plant is highly cultivated. The plant bears edible and highly nutritional fruit, which may be yellowish green, yellow or orange in colour when ripe. Seeds are numerous, black at maturity and rich in oil, lipids and proteins, which makes it crucial that seeds are defatted before use as adsorbent [20]. It is mainly produced for the juice and jams preparation or for consumption as fresh fruit. Great amount of papaya waste (peels) is generated due to high annual consumption in the industrialization process [21]. The chemical composition of papaya peel is crude fibre % (9.67), crude protein (6.89), fat % (0.33), Ca, Na, K, P, Mg, V-A, V-C, riboflavin, thiamine, niacin, phenol % (0.17), alkaloids % (0.39), flavonoids % (0.33), tannin % (0.35) and saponin % (0.49) [22]. Peels are occasionally used for animal feed and usually they are considered as waste and disposed, producing phytopathogens that pose risks to human health and cause ecological problems [23]. So far papaya peels are largely used as an ingredient in commercial skin care products and home-based skin care. However, in some recent studies powdered papaya peels and their chemically synthesized products have been found as potential adsorbent for the removal of various environmentally hazardous pollutants [24–27].

Thus keeping the toxicity of metal ions and adsorption ability of papaya peel in view, it was considered worthwhile to convert papaya peel into its carbon and use the material as papaya peel carbon (PPC) for the removal of Pb(II), Cu(II) and Ni(II) ions from the aqueous solutions. In the present work, attempts have been made for the batch and bulk removal of undertaken metals from their respective solutions and efficacy of the developed adsorbent has been established.

2. Materials and methods

2.1. Materials

All the reagents used were of analytical (AR) grade. Prior to use all glassware were nicely washed and cleaned. Nitrate salts of metal ions [$Pb(NO_3)_2$, $Ni(NO_3)_2{\cdot}6H_2O$, $Cu(NO_3)_2$] were purchased from M/s Merck, India. Sodium chloride (NaCl), sodium hydroxide (NaOH), hydrochloric acid (HCl), potassium chloride (KCl), sulphuric acid (H_2SO_4) and formic acid (HCOOH) were procured from M/s Sigma-Aldrich, (India). Throughout the study, laboratory prepared double distilled water was used. All readings were taken in triplicate.

2.2. Adsorbent preparation

Papaya peels, collected from the local market, were thoroughly washed with distilled water to remove particulate matter and were sun dried for 8 d. Dried papaya peels were cut into pieces and finely ground. These were once again washed with double distilled water to make the adsorbent free from colour, odour and other impurities. The material was further dried in oven at 60°C, crushed into fine powder and stored. The fine powdered sample was taken in silica crucible and kept in muffle furnace at 700°C for 30 min. The carbon so obtained was cooled in the desiccators. It was then ground, sieved to 50 mesh size and stored in desiccator till further use.

2.3. Characterization and instrumentation

Concentrations of Pb(II), Cu(II) and Ni(II) in the aqueous solutions were measured by atomic absorption spectroscopy (AAS) (Model: GBC902, M/s GBC Scientific Equipment, Australia). Surface morphology of PPC was examined by scanning electron microscopy equipped with energy dispersive X-ray spectroscopy (SEM/EDX, model-JSM, 6510 LV, M/s JEOL, Japan) at 1,500 magnification. Functional groups present in PPC and Pb(II) loaded PPC were determined using Fourier transformed infrared spectroscopy (Model: Nicolet iS50 FT-IR, M/s Thermo Fisher Scientific, USA) in the range of 4,000–400 cm^{-1} using KBr pellet technique. pH meter (Model Elico LI-120, M/s Elico, India) was used to monitor pH of the solution.

2.4. Point of zero charge determination

To determine the surface charge of the PPC, point of zero charge (pH_{zpc}) was investigated. In 100 mL flasks 20 mL of

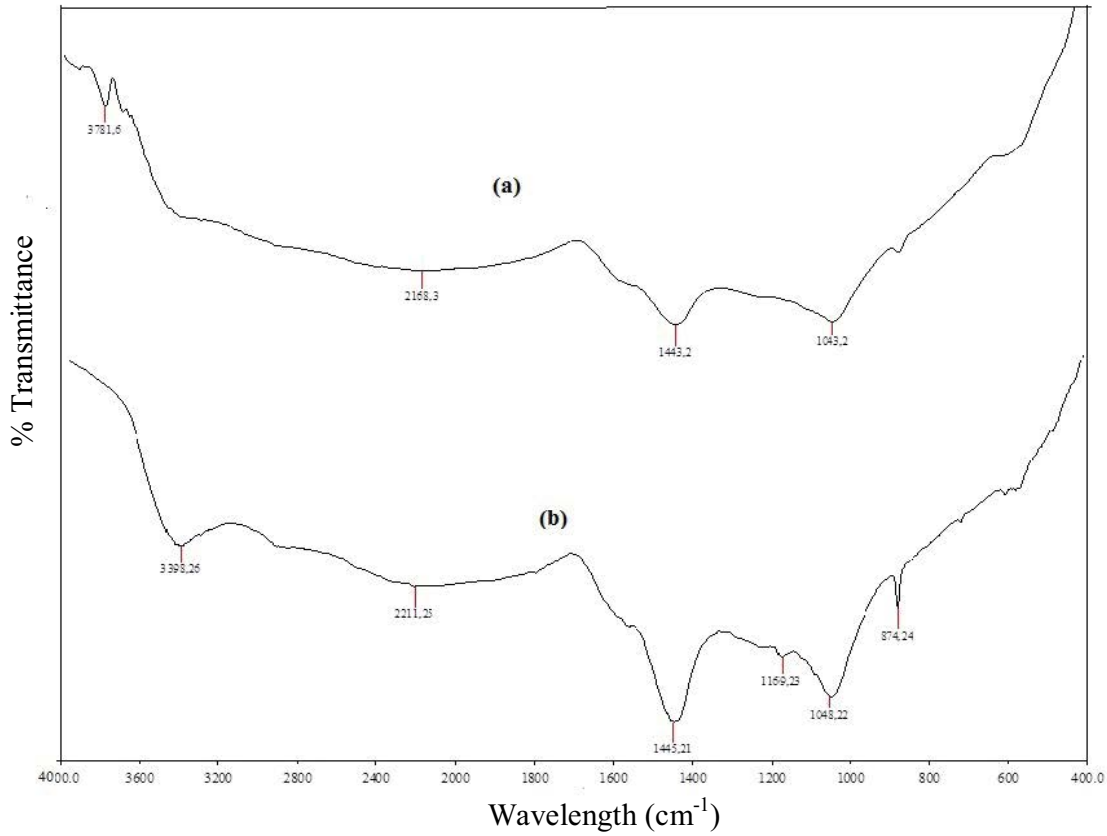

Fig. 1. FTIR spectra of PPC (a) before adsorption and (b) after adsorption of Pb(II).

0.1 M KCl was taken and 0.2 g of the adsorbent was then added to each solution. Totally 10 such flasks were taken and initial pH of each solution was adjusted between 2 and 12 using HCl and NaOH. After 24 h, pH of each solution was measured and difference in their pHs was recorded [28].

2.5. Batch adsorption studies

During batch adsorption studies, effects of various experimental parameters such as contact time, pH of solution, concentration of metal ions, adsorbent dosage and temperature on the adsorptive removal of adsorbate ions were studied. In each batch experiment, 20 mL of metal ion solution of 50 mg L^{-1} concentration and 0.2 g of PPC was taken in a closed 250 mL standard flask at a constant temperature. Kinetic studies were carried out at different initial metal ions concentrations using a fixed amount of PPC and agitated for a predetermined period. Using 0.5 M NaOH and 0.5 M HCl solutions pHs of working samples were adjusted. After completion of adsorption process, solution was filtered using Whatman filter paper 1.

The adsorption efficiency (%) of adsorbent and adsorbed amount of metal ions at equilibrium, q_e (mg g^{-1}), were calculated using the following equations (Eqs. (1) and (2)), respectively:

$$\% = \frac{C_i - C_e}{C_i} \times 100 \quad (1)$$

$$q_e = \frac{C_i - C_e}{m} \times V \quad (2)$$

where C_i and C_e are the concentrations (mg L^{-1}) of metal ion at initial and equilibrium, respectively. V is the volume (L) of the solution and m is the weight (g) of PPC.

2.6. Desorption and regeneration studies

In order to make the process more economical, feasible and commercially viable, desorption and regeneration studies were also carried out. Desorption and regeneration studies for Pb(II), Ni(II) and Cu(II) were carried out by batch adsorption mode using various desorbing agents such as 0.1 M of HCl, NaOH, CH_3COOH, H_2SO_4 and HNO_3 solution.

3. Results and discussions

3.1. Chemical characterization of PPC

3.1.1. Scanning electron microscopy

SEM photographs of PPC reveal a more prominent porous and irregular texture surface morphology. After adsorption, a comparatively smoother surface is obtained which is due to filling of Pb(II) in the porous PPC, indicating thereby metal ion adherence onto the surface of adsorbent material.

3.1.2. Elemental analysis

To explain the behaviour of adsorbent during the adsorption process, study of chemical composition becomes very important. Table 1 presents the results of elemental analysis of PPC before and after Pb(II) adsorption. These results clearly reflect significant contents of carbon in the PPC due to high carbonization temperature. High percentage of carbon (67.27%) present in the adsorbent is responsible for greater amount of adsorption of heavy metal ions from its aqueous solution. Presence of Pb(II) after adsorption clearly confirms the successful adsorption of Pb(II) over PPC.

3.1.3. FTIR analysis

Fig. 1 presents FTIR spectra of PPC (a) before adsorption of Pb(II) and (b) after adsorption of Pb(II). Peaks obtained at 3,781.6 and 3,398.26 cm^{-1} corresponding to the –OH group and or moisture and a peak in the spectrum at 3,398.26 cm^{-1} shows the presence of intermolecular hydrogen bond with –OH group [29]. The absorption band at 3,781.6 cm^{-1} reveals the presence of stretching vibration of O–H on PPC, which diminishes after adsorption with Pb(II) and is shifted to lower wave number 3,398.26 cm^{-1}. This reflects the formation of hydrogen bond [30]. The peak at 3,398.26 cm^{-1} is due to the presence of alcohols, chemisorbed water and phenols that is present on both lignin and cellulose in PPC. Peak at 3,398.26 cm^{-1} is broad due to the complex stretching vibrational modes bands of –OH group in chemisorbed water and hydrogen bonding. The vibrational mode in this area also corresponds to intra and intermolecular hydrogen bonding [31]. Shift in the peak from 2,168.3 to 2,211.25 cm^{-1} is attributed to C–C stretching. Bands at 1,443.2 and 1,445.21 cm^{-1} show C–H bending. The peak at 1,169.23 cm^{-1} corresponds to C–O asymmetric stretching [32], while the peak at 874.24 cm^{-1} is associated with carbonate group internal C–O vibrations [33].

3.2. Effect of initial concentration

The initial metal ion concentration plays a significant role in the adsorption process. Effect of initial metal ion concentration on the adsorption process was examined at different dye concentrations, ranging from 20 to 100 mg L^{-1} with a contact time of 180 min, pH 5 for Cu(II) and pH 6 for Pb(II) and Ni(II) ions, at temperature 313 K and 0.5 g dosage of PPC. It was found that the adsorption on PPC surface decreased from 99% to 90.64% for Pb(II), 99.36% to 89.06% for Cu(II) and 97.86% to 84.31% for Ni(II), respectively, as the initial concentration of metal ion in each solution was increased from 20 to 100 mg L^{-1} (Fig. 2). This is due to the fact that at low initial concentration of metal ion, there is large availability of adsorption sites on the PPC surface, while with the increase in the concentration of metal ion coverage area decreases [34].

Table 1
Elemental analysis of PPC

Element	Percentage before Pb(II) adsorption	Percentage after Pb(II) adsorption
Carbon	60.00	60.00
Oxygen	25.69	24.67
Phosphorus	3.03	3.03
Potassium	1.43	1.43
Calcium	8.80	8.80
Lead		1.02

3.3. Effect of contact time

The effect of contact time was studied in the range of 5–180 min at 30°C and initial concentration of each metal ion was 50 mg L^{-1}. The pH 6 solutions were taken for both Pb(II) and Ni(II) ions, while for Cu(II) ions the pH was kept 5. Evolution of the adsorbed amount of metal ions with the contact time presented in Fig. 3 reflects that for all the three metal ions, initially rate of adsorption was fast and slows down with time to attain equilibrium in about 180 min. It was observed that once the equilibrium was established no significant adsorption of metal ions was observed. Fig. 3 shows the kinetic regions characterized by a high adsorption rate due to higher initial number of available sites of PPC and the greater driving force for mass transfer. During initial stage, metal ions easily occupy the adsorption sites, while with progress of time, there is decrease in the number of free sites and the adsorption capacity is limited due to the assembled non-adsorbed cations in solution [35].

3.4. Effect of pH

The adsorptive removal of heavy metal ions from their aqueous solutions is highly dependent on the solution pH [36]. The pH of the solution has a significant impact on the uptake of heavy metal ions as it determines the degree of ionization, speciation and surface charge of the adsorbent. Influence of pH on adsorption of metal ions was evaluated by experiments in the pH range of 2–7 for Pb(II), 2–8 for Cu(II) and 2–10 for Ni(II). These pH ranges were chosen

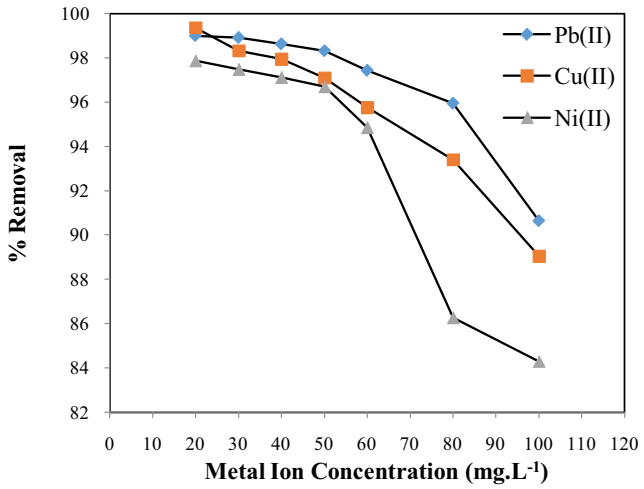

Fig. 2. Effect of concentration of metal ions on the adsorption over PPC.

in order to avoid precipitation of metal ions in the form of three metal hydroxides. Fig. 4 presents the effect of pH on the adsorption of metal ions and the optimum pH for Pb(II) and Ni(II) was found to be 6, while for Cu(II) it was 5. This indicates that in each case the positive charge on adsorbent surface leads to unfavourable cations adsorption at lower pH. At lower pH, hydrogen ions compete strongly with metal ions for the active sites and so lower adsorption is observed. At high pH, the surface of the adsorbent has higher negative charge, which causes higher cations attraction. It is also evident that at very high pH, the precipitation of metal ions takes place, which makes their separation through adsorption impossible [37].

The pH shows the ionic state of functional groups, adsorbent surface properties (e.g. pHz) and aqueous metal speciation, respectively. The point of zero charge (pHz) can be described as the pH with which net total surface charge is zero. Surface of the adsorbent is positively charged below pHz, otherwise it is negatively charged. PPC shows a zero surface charge for Pb(II) at pH 6, for Cu(II) at pH 4.8 and for Ni(II) at pH 5.9, respectively. Hence, to achieve high adsorption of metal ions onto PPC without metal hydroxide precipitation, pH of 6.0 for Pb(II) and Ni(II) and pH of 5 for Cu(II) were selected for the entire experimental work.

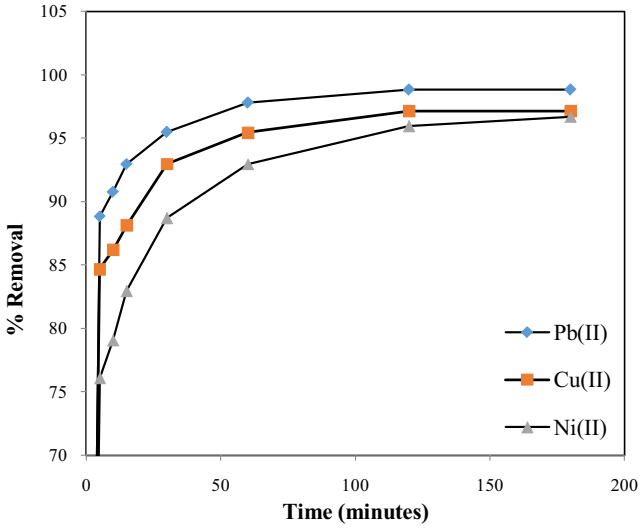

Fig. 3. Effect of contact time on the adsorption of metal ions over PPC.

3.5. Effect of adsorbent dosage

Optimum adsorption capacities for Pb(II), Cu(II) and Ni(II) ions have been found as 9.718, 9.326, 8.647 mg/g, respectively. The adsorption capacity (mg g^{-1}) of Pb(II), Cu(II) and Ni(II) at different dosages of PPC is shown in Fig. 5 and it was found that the adsorption capacity decreases with increase in adsorbent dosage. This may be due to the fact that some adsorption sites may remain unsaturated during the adsorption process whereas the number of sites available for adsorption increases with increasing adsorbent dosage, which results in the increase of percentage removal and decrease in adsorption capacity [38].

3.6. Adsorption isotherms

Adsorption isotherm plays an important role in designing adsorption systems and gives significant information about the amount of adsorbent required for the removal of metal ions from their aqueous solutions. According to Langmuir model, uptake of metal ions occur on a homogeneous surface by monolayer adsorption without any interaction between adsorbed ions and the adsorption of each molecule onto the surface of adsorbent has equal adsorption activation energy. The well-known linear form of Langmuir isotherm equation [39] is given as

$$\frac{1}{q_e}=\frac{1}{q_m}+\frac{1}{bq_mC_e} \tag{3}$$

where q_e is the equilibrium capacity of metal ion on the adsorbent (mg g^{-1}), C_e is the equilibrium concentration of

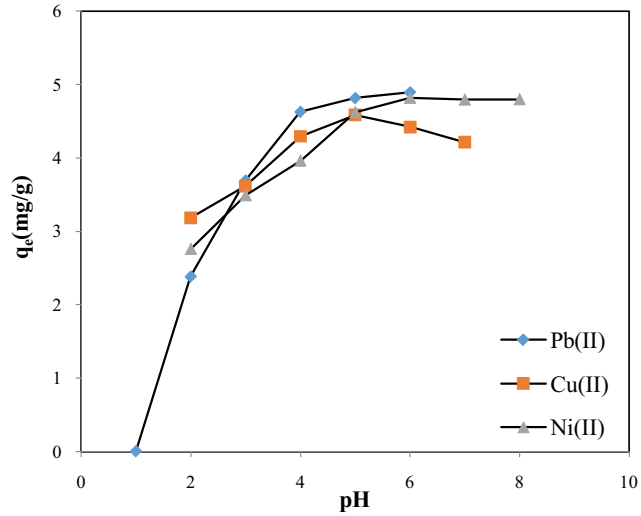

Fig. 4. Effect of pH on the adsorption of metal ions over PPC.

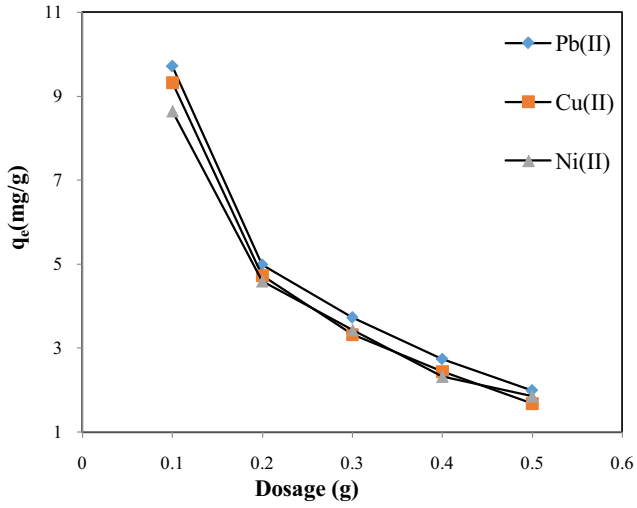

Fig. 5. Effect of dosage of PPC on the adsorption of metal ions.

metal ion solution (mg L^{-1}), q_m is the monolayer adsorption capacity of the adsorbent (mg g^{-1}), and b is the Langmuir constant (L mg g^{-1}). A plot of $1/q_e$ vs. $1/C_e$ is shown in Fig. 6 and values obtained are given in Table 2.

Freundlich isotherm is applied for multilayer adsorption on heterogeneous adsorbents and it is assumed that adsorption sites increase exponentially with respect to heat of adsorption. The linear form of Freundlich equation [40] is given as:

$$\log q_e = \log K_f + \left(\frac{1}{n}\right)\log C_e \tag{4}$$

where $1/n$ and K_f (mg g^{-1})(L $mg^{-1})^{1/n}$ are Freundlich constants related to adsorption intensity and adsorption capacity, respectively. The plot of $\log q_e$ vs. $\log C_e$ at 30°C is presented in Fig. 7 and the values of correlation coefficient (R^2) and the constant are given in Table 2. The values of n and R^2 predict the favourability and feasibility of adsorption isotherm.

Temkin and Pyzhev isotherm [41] was studied to analyse the adsorbent–adsorbate interaction and heat of adsorption. The linear form of Temkin isotherm equation is given as:

$$q_e = B_1 \ln K_t + B_1 \ln C_e \tag{5}$$

where $B_1 = RT/b$, R is the universal gas constant (8.314 J K mol^{-1}), T is the absolute temperature in K, B_1 (J mol^{-1}) is related to heat of adsorption and K_t (L mg^{-1}) is the equilibrium binding constant. A plot of q_e vs. $\ln C_e$ is shown in Fig. 8 and values of constant are given in Table 2.

Adsorption process was also verified by Dubinin–Radushkevich (D-R) adsorption isotherm model [42]. This model does not assume constant adsorption potential or homogeneous surface and is described by the following equations:

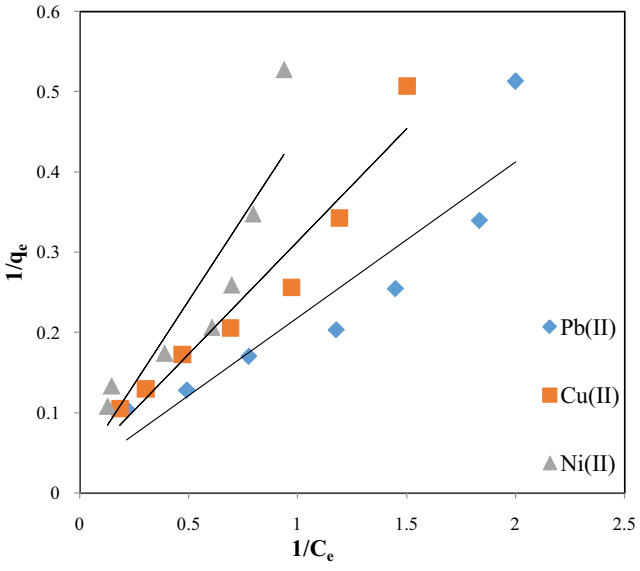

Fig. 6. Langmuir adsorption isotherms for the adsorption of metal ions over PPC.

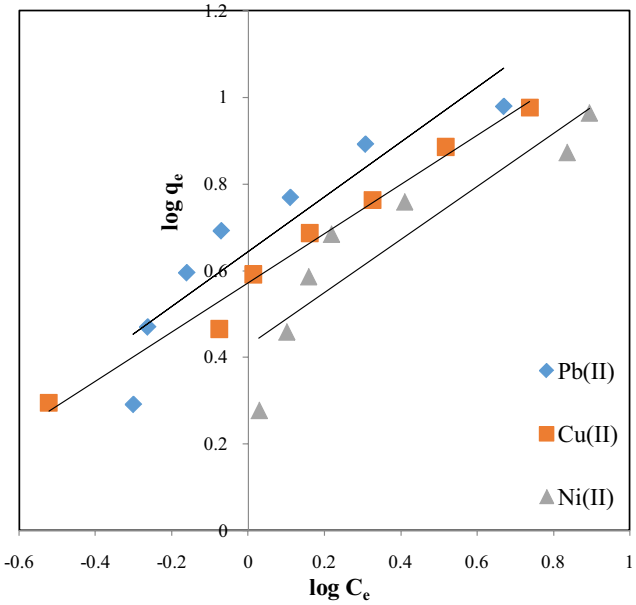

Fig. 7. Freundlich adsorption isotherms for the adsorption of metal ions over PPC.

Table 2
Langmuir, Freundlich, Temkin and D-R constants for adsorption of metal ions over PPC

	Pb(II)	Cu(II)	Ni(II)
Langmuir isotherm			
q_m (mg g^{-1})	40.983	38.012	32.258
b (L mg^{-1})	7.959	1.052	13.467
R^2	0.848	0.946	0.812
RMSE	0.043	0.042	0.044
χ^2 (Chi square)	0.000	5.95E-05	0.000
Freundlich isotherm			
K_f ($mg^{(1-n)}$ L^n g^{-1})	4.394	3.731	2.668
$1/n$	0.6322	0.5668	0.6124
R^2	0.850	0.983	0.826
RMSE	0.028	0.023	0.027
χ^2 (Chi square)	0.001	0.002	0.001
Temkin isotherm			
K_t (L mg^{-1})	4.539	4.634	2.242
B_1 (J mol^{-1})	3.280	2.680	3.055
R^2	0.966	0.917	0.934
RMSE	0.564	0.523	0.432
χ^2 (Chi square)	0.054	0.089	0.076
D-R isotherm			
q_m (mg g^{-1})	9.685	6.501	8.922
β (mol^2 K J^{-2})	2×10^{-7}	1×10^{-7}	5×10^{-7}
R^2	0.969	0.743	0.965
RMSE	0.342	0.332	0.434
χ^2 (Chi square)	0.022	0.012	0.011

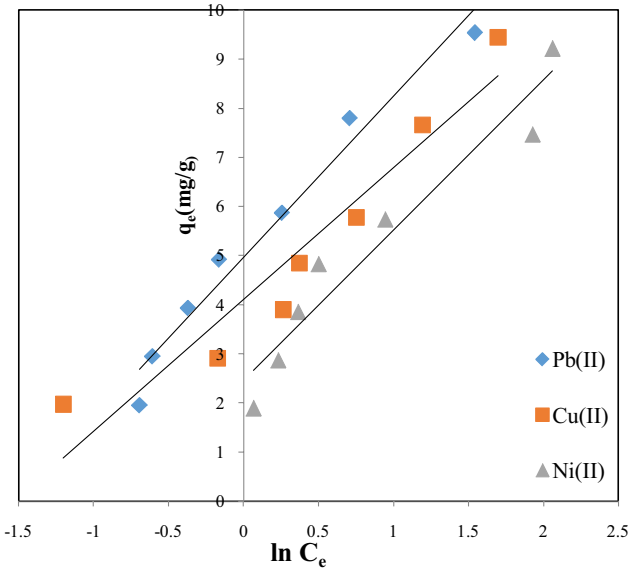

Fig. 8. Temkin adsorption isotherms for the adsorption of metal ions over PPC.

$$\ln q_e = \ln q_m - \beta\varepsilon^2 \tag{6}$$

$$E = \frac{1}{\sqrt{-2\beta}} \tag{7}$$

where ε is the Polanyi potential, which is equal to [RT ln 1 + (1/C_e)], where T is the absolute temperature in Kelvin and R (8.314 J mol^{-1} K^{-1}) is the gas constant, q_m (mg g^{-1}) is the theoretical saturation capacity and β (mol^2 K J^{-2}) is an isotherm constant related to parameter E (mean free energy) per mole of adsorbate (kJ mol^{-1}). A plot of ln q_e vs. ε^2 was drawn (Fig. 9) and values of various constants are calculated, which are presented in Table 2.

The adsorption isotherm studies reveal that Pb(II) and Ni(II) ions follow D-R isotherms, while adsorption of Cu(II) ions is governed by Freundlich isotherm. The Freundlich type adsorption isotherm demonstrates surface heterogeneity of the adsorbent. This indicates that the surface of the adsorbent is made up of small heterogeneous adsorption patches, which are very much similar to each other in adsorption capability [30].

3.7. Adsorption kinetics

The nature of adsorption process depends on physical/chemical characteristics of system and respective conditions. The rate and mechanism of adsorption process were investigated by the kinetic models such as pseudo-first-order, pseudo-second-order, Elovich model and intraparticle diffusion, respectively [43]. The following mathematical expression describes pseudo-first-order model:

$$\log\left(q_e - q_t\right) = \log q_e - \frac{k_1}{2.303} \times t \tag{8}$$

where q_e (mg g^{-1}) is the adsorption capacity at equilibrium and q_t (mg g^{-1}) is the amount of metal adsorbed at any time t (min) and k_1 (min^{-1}) is the pseudo-first-order rate constant.

Pseudo-second-order model is expressed as:

$$\frac{t}{q_t} = \frac{1}{k_2 q_e^2} + \frac{t}{q_e} \tag{9}$$

where k_2 (g mg^{-1} min^{-1}) is the pseudo-second-order rate constant. For different concentrations, the values of q_e, k_1 and k_2 were calculated from their respected plots and results are shown in Table 3. The data show that the values of correlation coefficient for pseudo-second-order are relatively higher than those for pseudo-first-order kinetic model. However, for pseudo-second-order kinetic model, it was observed that the experimental q_e values are very close to the calculated q_e values. This study shows that the adsorption of Pb(II), Cu(II) and Ni(II) could be best described by the pseudo-second-order model.

Intraparticle diffusion can be estimated by using the Weber–Morris intraparticle diffusion model:

$$q_e = k_{id}\left(t\right)^{1/2} + C \tag{10}$$

where k_{id} (g mg^{-1} min$^{-1/2}$) is the intraparticle diffusion rate coefficient and C gives an idea about the thickness of the boundary layer. These values were determined by a plot of q_t vs. $t^{1/2}$. The deviation of the straight lines is due to the difference between final mass transfer rate and initial mass transfer rate, respectively. This deviation also shows that the pore diffusion is not the sole rate-controlling step [44]. The k_{id} values of different metal ions are presented in Table 3.

Elovich kinetic model was developed by Zeldowitsch assuming that the actual solid adsorbent surfaces are energetically heterogeneous and there is no interaction among the adsorbed species. The Elovich equation is expressed as:

$$q_t = A + B\ln\left(t\right) \tag{11}$$

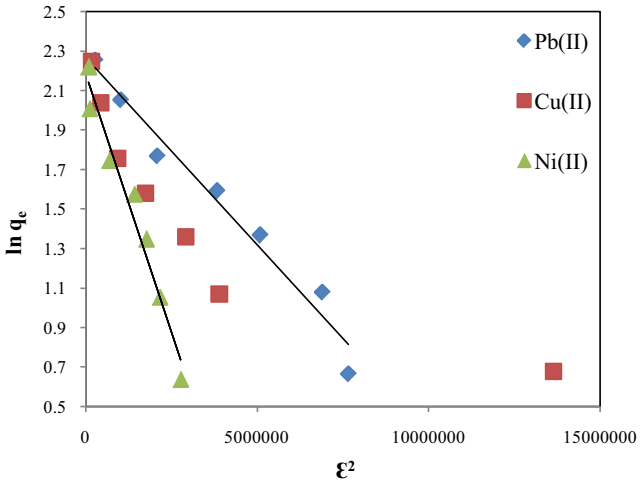

Fig. 9. D-R adsorption isotherms for the adsorption of metal ions over PPC.

where A (L mg^{-1}) and B (J mol^{-1}) are Elovich constants. The values of A, B and R^2 were calculated from the plot of q_t vs. ln$t$ and values are given in Table 3. It is evident from the table that the experimental data are best followed by pseudo-second-order kinetics for Pb(II), Cu(II) and Ni(II) adsorption. In addition, the calculated values of q_e obtained from pseudo-second-order model were much close to the experimental q_e values. This, however, showed that the adsorption kinetic process fitted well with the pseudo-second-order rate equation, which indicated that the overall process was controlled by chemisorption and involved valence forces through sharing or exchange of electrons between adsorbate and adsorbent [45]. Non zero values of C further indicate that the ongoing adsorption involves a complex process and intraparicle diffusion is not the sole rate-determining step. The plot of intraparticle diffusion model shows multilinearity of adsorbate adsorption, implying that two or more steps are participating in adsorption process. First linear portion is attributed to external diffusion, while second linear stage ascribed to the intraparticle diffusion as a delayed process and the third linear portion shows equilibrium establishment [45].

Table 3
Kinetic parameter on the adsorption of Pb(II), Cu(II) and Ni(II)

	Pb(II)	Cu(II)	Ni(II)
Pseudo-first-order			
q_e^{cal} (mg g^{-1})	1.089	1.091	1.270
q_e^{exp} (mg g^{-1})	4.942	4.857	4.835
k_1 (min^{-1})	0.072	0.055	0.033
R^2	0.953	0.971	0.983
RMSE	0.431	0.332	0.437
χ^2 (Chi square)	0.002	0.001	0.006
Pseudo-second-order			
q_e^{cal} (mg g^{-1})	4.965	4.892	4.887
q_e^{exp} (mg g^{-1})	4.942	4.857	4.835
k_2 (g mg^{-1} min^{-1})	0.228	0.157	0.083
R^2	1	1	1
RMSE	0.431	0.342	0.344
χ^2 (Chi square)	0.005	0.009	0.012
Intraparticle diffusion			
k_{id} (mg g^{-1} min$^{-1/2}$)	0.035	0.047	0.076
C (mg g^{-1})	4.488	4.247	3.834
R^2	0.790	0.812	0.846
RMSE	0.528	0.431	0.342
χ^2 (Chi square)	0.003	0.008	0.021
Elovich			
A (L mg^{-1})	4.262	3.950	3.368
B (J mol^{-1})	0.136	0.180	0.287
R^2	0.941	0.944	0.967
RMSE	0.315	0.335	0.432
χ^2 (Chi square)	0.023	0.020	0.031

3.8. Thermodynamic parameters

The isothermal model such as Langmuir proves their utility in the determination of thermodynamics of the adsorption process. Using Langmuir adsorption data, particularly the Langmuir constant, energy of adsorption (b), various thermodynamic parameters of the adsorption systems such as change in Gibb's free energy ($\Delta G°$), change in enthalpy ($\Delta H°$) and change in entropy ($\Delta S°$) are calculated from the following well-known relations [46]:

$$K_c = \frac{C_a}{C_e} \tag{12}$$

$$\Delta G° = -RT \ln K_c \tag{13}$$

where, K_c is the equilibrium constant, C_a (mg L^{-1}) is the solid phase concentration at equilibrium and C_e (mg L^{-1}) is the equilibrium concentration in solution, R is the gas constant (J K^{-1} mol^{-1}) and T is Kelvin temperature of the working solution.

$$\log K_c = \frac{\Delta S°}{2.303R} - \frac{\Delta H°}{2.303RT} \tag{14}$$

Values of $\Delta S°$ and $\Delta H°$ were obtained from the intercept and slope of the plot logK_c vs. 1/T as shown in Fig. 10 and presented in Table 4. Negative values of $\Delta G°$ show the adsorption of Pb(II), Ni(II) and Cu(II) metal ions onto PPC as spontaneous and thermodynamically favourable processes. Positive values of $\Delta H°$ obtained for the adsorption of Pb(II), Cu(II) and Ni(II) ions indicate the endothermic nature of each adsorption process. In each case, negative values of $\Delta G°$ also confirm the spontaneous nature of the reaction, while the positive value for $\Delta S°$ indicate increase in the randomness at the solid–solution interface during the adsorption process of Pb(II), Cu(II) and Ni(II) metal ions. At high temperature, values of $\Delta G°$ become more negative that shows greater driving force for adsorption. The positive values of $\Delta S°$ obtained for Pb(II), Cu(II)

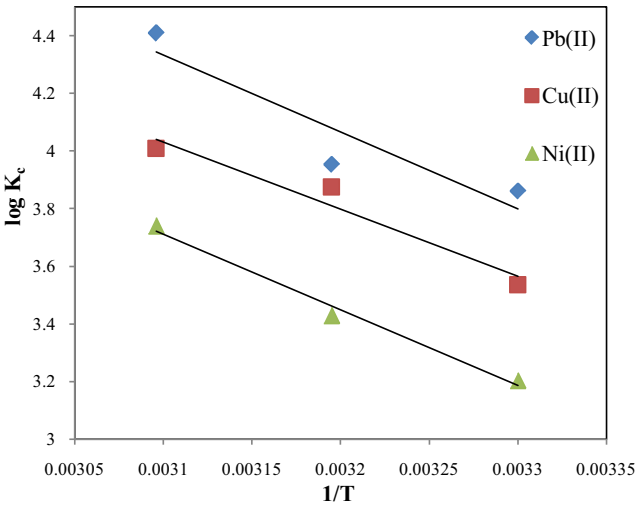

Fig. 10. logK_c vs. 1/T graph verifying Van't Hoff equation.

and Ni(II) ions reflect increased spontaneous nature of the adsorption.

The nature of adsorption is explained by the magnitude of activation energy. Two types of adsorption can occur, physical or chemical. Chemical adsorption involves forces much stronger than those of physical adsorption and is specific. The chemical adsorption has activation energy of the same magnitude as the heat of chemical reaction. However, physical adsorption is easily reversible and due to small energy requirements equilibrium is attained rapidly. Usually, activation energy for physical adsorption is not much as forces involved here are weak. The plot of $\ln K_c$ vs. $1/T$ is shown in Fig. 11. The slope of linear plot gives corresponding activation energy which was determined by Arrhenius equation:

$$\ln K_c = \frac{E_a}{RT} + \ln K_0 \tag{15}$$

The value of activation energy for Pb(II), Cu(II) and Ni(II) was found to be 22.183, 19.367 and 21.808 kJ mol^{-1}, respectively. The values of activation energy obtained for different metal ions confirm that the adsorption mainly occurs through physisorption.

3.9. Desorption and regeneration studies

Desorption of adsorbent plays a very important role in practical application of wastewater treatment. Desorption studies were performed using different eluents such as HCl, HCOOH, HNO_3, H_2SO_4 and NaOH in 20 mL Pb(II), Cu(II) and Ni(II) solution. The initial concentration of 50 mg L^{-1} of different metal ions was treated separately with 0.2 g of adsorbent. After 24 h, the solution was filtered and the filtrate was analysed for residual concentration. The adsorbent was washed several times with double distilled water to ensure complete removal of metal ions and then it was treated with 20 mL of desorbing eluents. The amount of Pb(II), Cu(II) and Ni(II) desorbed in the eluent solution was analysed by AAS. The graph for desorption is shown in Fig. 12.

It is evident from results that a dominant protonation reaction occurred between H^+ ions and active sites due to abundant H^+ ions in the solution. Complexation between the active sites and metal ions was prevented, and metal ions precipitate gets dissolved [47]. Amongst the mediums used, 0.1 M HNO_3 was found to be good enough for desorbing more than 85% of Pb(II), 0.1 M HCl for desorbing more than 80% of the adsorbed Cu(II) and Ni(II) from

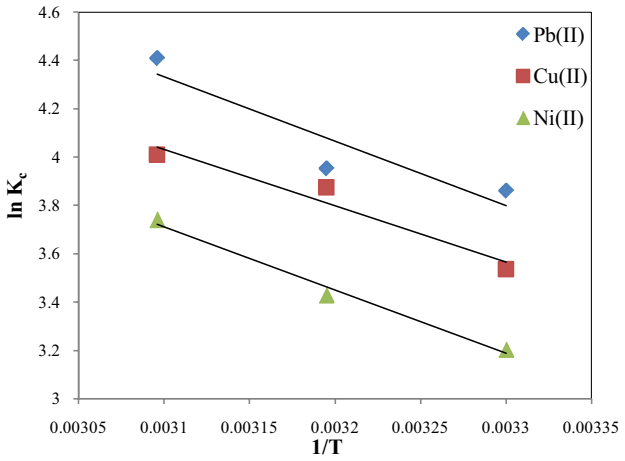

Fig. 11. $\ln K_c$ vs. $1/T$ graph verifying Arrhenius equation.

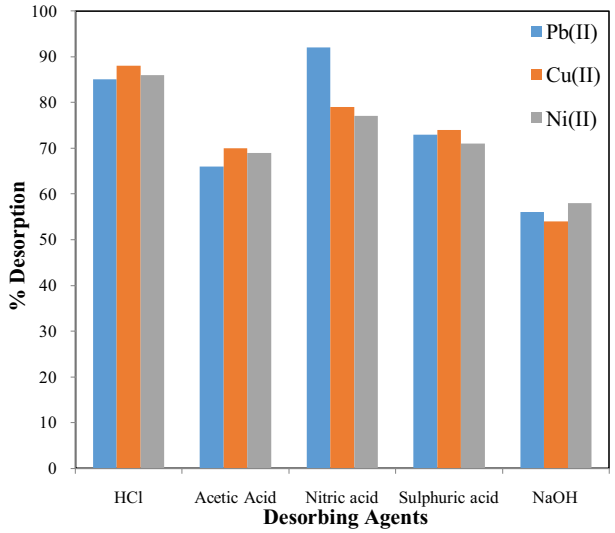

Fig. 12. Desorption of metal ions with different eluents.

Table 4
Thermodynamic parameters for the adsorption of Pb(II), Cu(II) and Ni(II) on PPC

Metal ion	Temperature (K)	$\Delta G°$ (kJ mol^{-1})	$\Delta H°$ (kJ mol^{-1})	$\Delta S°$ (kJ mol^{-1} K^{-1})
	303	–9.727		
Pb(II)	313	–10.291	22.109	0.104
	323	–11.840		
	303	–8.905		
Cu(II)	313	–10.764	19.300	0.093
	323	–10.764		
	303	–8.072		
Ni(II)	313	–8.923	21.810	0.226
	323	–10.043		

the spent adsorbent. The reusability was checked by following the adsorption–desorption process for five cycles for Pb(II) ions and the adsorption efficiency in each cycle was studied. Almost 92%, 83%, 71%, 65% and 54% of Pb(II) ions were recovered, from 1st to 5th cycle, respectively. In this study, reusability of the adsorbent was checked with Pb(II) ions as they were well desorbed from the adsorbent. The PPC adsorbent kept its adsorption capability even after repeated adsorption–regeneration cycles with only small changes; this indicates that there are almost no irreversible sites on the surface of PPC. The recyclability studies suggest that these PPC can be repeatedly used as an efficient adsorbent in wastewater treatment.

3.10. Adsorption mechanism

It is evident from FTIR spectra that there is a strong electrostatic interaction between Pb(II) and the active sites of PPC (–OH and C–O–C groups) or chelation via hydrogen bond formation. SEM image of Pb(II)-loaded PPC suggests the massive adsorption of Pb(II) onto the porous surface of PPC as evident from the smooth surface after loaded with Pb(II). The pH effect also indicates the existence of electrostatic interaction between adsorbate and adsorbent. Kinetic studies indicate that the rate determining step in adsorption process is physisorption with other processes such as surface adsorption or, film diffusion or external diffusion might also be involved. Desorption studies reveal the involvement of ion exchange. Thermodynamic studies showed that the physical adsorption is involved in the adsorption process. Therefore, overall there is involvement of physical forces (electrostatic interaction, chelation, ion exchange and adsorption process) in the sequestration of Pb(II) from aqueous solution using PPC [48,49].

3.11. Comparison with other adsorbents

The monolayer adsorption capacity (q_m) values of 40.98 mg g^{-1} for Pb(II), 38.02 mg g^{-1} for Cu(II) and 32.25 mg g^{-1} for Ni(II) observed in this study have been compared well with some other adsorbents reported from literature as shown in Table 5. By comparing the data, it can be safely concluded that PPC can be utilized simultaneously for the removal of Pb(II), Cu(II) and Ni(II) from their aqueous solutions and exhibit excellent adsorption capacity with each metal ion.

4. Conclusion

In this study, PPC was employed as an effective low-cost adsorbent for the removal of Pb(II), Cu(II) and Ni(II) ions from wastewaters. Optimum adsorption conditions for Pb(II), Cu(II) and Ni(II) were determined as a function of contact time, pH, initial metal ion concentration, adsorbent dosage and temperature of solution. For Pb(II) and Ni(II), the maximum adsorption was achieved at pH 6, while for Cu(II) it was pH 5. In each case, adsorption equilibrium could be attained in 180 min. D-R adsorption isotherm model best described adsorption of Pb(II) and Ni(II) ions onto PPC whereas Freundlich adsorption

Table 5
Comparison with other adsorbents for the removal of Pb(II), Cu(II) and Ni(II)

Adsorbate	Adsorbent	q_m (mg g^{-1})	Reference
Pb(II)	Papaya peel carbon	40.98	This work
Cu(II)	Papaya peel carbon	38.02	This work
Ni(II)	Papaya peel carbon	32.25	This work
Cu(II)	Defatted papaya seed	17.29	[20]
Pb(II)	Defatted papaya seed	53.02	[20]
Cu(II)	Poly flavanoid tannins	8.78	[50]
Cu(II)	Olive stone–activated carbon	17.83	[51]
Pb(II)	Poly flavanoid tannins	31.32	[50]
Pb(II)	Olive stone–activated carbon	22.37	[51]
Ni(II)	Dolomite powder	5.41	[52]
Pb(II)	Cellu/cys-bent nanocomposite	18.52	[53]
Cu(II)	Cellu/cys-bent nanocomposite	32.36	[53]
Cu(II)	Poly (methyl methacrylate)-grafted alginate/Fe_3O_4 nanocomposite	35.71	[48]
Pb(II)	Groundnut husk modified with guar gum (GG)	9.76	[54]
Cu(II)	Groundnut husk modified with guar gum (GG)	9.26	[54]
Ni(II)	Groundnut husk modified with guar gum (GG)	6.74	[54]
Cu(II)	*Luffa acutangula* modified Tetraethoxysilane (LAP-TS)	22.05	[38]
Ni(II)	Luffa acutangula modifified Tetraethoxysilane (LAP-TS)	22.71	[38]
Pb(II)	Pistachio shell carbon (PSC)	24.0	[55]
Pb(II)	CTAB/MMT nanocomposite	4.73	[28]

isotherm described adsorption of Cu(II). The maximum monolayer adsorption capacity (q_m) was found to be 40.98, 38.02 and 32.25 mg g^{-1} for Pb(II), Cu(II) and Ni(II) ions, respectively. The pseudo-second-order model was found to be best fitted with highest correlation coefficients (R^2). The positive value of $\Delta H°$ indicates the reaction to be endothermic in nature. While the positive value of $\Delta S°$ indicates randomness at solid–liquid solutions interface during adsorption of Pb(II), Cu(II) and Ni(II) ions. Desorption and regeneration study shows that PPC is an efficient and potential adsorbent. It can be concluded that PPC is an effective, alternative and low-cost adsorbent for the removal of Pb(II), Cu(II) and Ni(II) metal ions from wastewater.

Acknowledgments

The authors are grateful to Chairman, Department of Applied chemistry, AMU; USIF, AMU, Aligarh and MNIT, Jaipur, for providing research facility. The authors AM and JM are thankful to Ministry of Human Resource Development, Government of India for funding SPARC project (SPARC/2018-2019/P307/SL).

References

[1] L.B. Franklin, Wastewater Engineering: Treatment, Disposal and Reuse, McGraw Hill, Inc., New York, 1991.
[2] U.N. Joshi, Y.P. Luthra, An overview of heavy metals: impact and remediation, Curr. Sci., 78 (2000) 773–775.
[3] H. Needleman, Lead poisoning, Annual Rev. Med., 55 (2004) 209–222.
[4] R.C. Gracia, W.R. Snodgrass, Lead toxicity and chelation therapy, Am. J. Health-Syst. Pharm., 64 (2007) 45–53.
[5] National Research Council, Copper in Drinking Water, National Academies Press, Washington, DC, 2000.
[6] https://www.who.int/water_sanitation_health/water-quality/guidelines/chemicals/ Nickel 110805.pdf?ua=1 (Nickel in Drinking-water Background document for development of WHO Guidelines for Drinking-water Quality)
[7] F. Fu, Q. Wang, Removal of heavy metal ions from wastewaters: a review, J. Environ. Manage., 92 (2011) 407–418.
[8] L.A. Malik, A. Bashir, A. Qureashi, A.H. Pandith, Detection and removal of heavy metal ions: a review, Environ. Chem. Lett., 17 (2019) 1495–1521.
[9] S. Wadhawan, A. Jain, J. Nayyar, S.K. Mehta, Role of nanomaterials as adsorbents in heavy metal ion removal from waste water: a review, J. Water Process Eng., 33 (2020) 101038.
[10] M. Gorgievsk, D. Bozic, V. Stankovic, N. Strbac, S. Snezana, Kinetics, equilibrium and mechanism of Cu^{2+}, Ni^{2+} and Zn^{2+} ions biosorption using wheat straw, Ecol. Eng., 58 (2013) 113–122.
[11] D. Bozic, M. Gorgievsk, V. Stankovic, N. Strbac, S. Snezana, N. Petrovi, Adsorption of heavy metal ions by beech sawdust – kinetics, mechanism and equilibrium of the process, Ecol. Eng., 58 (2013) 202–203.
[12] I. Anastopoulos, G.Z. Kyzas, Progress in batch biosorption of heavy metals onto algae, J. Mol. Liq., 209 (2015) 77–86.
[13] I. Anastopoulos, A. Bhatnagar, D.N. Bikiaris, G.Z. Kyzas, Chitin adsorbents for toxic metals: a review, Int. J. Mol. Sci., 18 (2017) 114.
[14] A. Mittal, M. Teotia, R.K. Soni, J. Mittal, Applications of egg shell and egg shell membrane as adsorbent: a review, J. Mol. Liq., 223 (2016) 376–387.
[15] A. Mittal, R. Ahmad, I. Hasan, Iron oxide–impregnated dextrin nanocomposite: synthesis and its application for the biosorption of Cr(VI) ions from aqueous solution, Desal. Water Treat., 57 (2016) 15133–15145.
[16] M. Naushad, A. Mittal, M. Rathor, V. Gupta, Ion-exchange kinetic studies for Cd(II), Co(II), Cu(II) and Pb(II) metal ions over a composite cation exchanger, Desal. Water Treat., 54 (2015) 2883–2890.
[17] H. Daraei, A. Mittal, M. Noorisepehr, J. Mittal, Separation of chromium from water samples using egg shell powder as a low-cost sorbent: kinetic and thermodynamic studies, Desal. Water Treat., 53 (2015) 214–220.
[18] H. Daraei, A. Mittal, J. Mittal, H. Kamali, Optimization of Cr(VI) removal onto biosorbent eggshell membrane: experimental and theoretical approaches, Desal. Water Treat., 52 (2014) 1307–1315.
[19] A. Mittal, R. Ahmad, I. Hasan, Biosorption of Pb^{2+}, Ni^{2+} and Cu^{2+} ions from aqueous solutions by L-cystein modified montmorillonite immobilized alginate nanocomposite, Desal. Water Treat., 57 (2016) 17790–17807.
[20] Z.N. Garba, I. Bello, A. Galadimaa, A.Y. Lawal, Optimization of adsorption conditions using central composite design for the removal of copper(II) and lead(II) by defatted papaya seed, Karbala Int. J. Mod. Sci., 2 (2016) 20–28.
[21] F.A. Pavan, E.S. Camacho, E.C. Lima, G.L. Dotto, V.T.A. Branco, S.L.P. Dias, Formosa papaya seed powder (FPSP): preparation, characterization and application as an alternative adsorbent for the removal of crystal violet from aqueous phase, J. Environ. Chem. Eng., 2 (2014) 230–238.
[22] K.S. Chukwuka, M. Iwuagwu, U.N. Uka, Evaluation of nutritional components of carica papaya l. At different stages of ripening, IOSR J. Pharm. Biol. Sci., 6 (2013) 13–16.
[23] P. Chaiwut, P. Pintathong, S. Rawdkuen, Extraction and three-phase partitioning behavior of proteases from papaya peels, Process Biochem., 45 (2010) 1172–1175.
[24] A.A. Bayode, F.O. Agunbiade, M.O. Omorogie, R. Moodley, O. Bodede, E.I. Unuabonah, Clean technology for synchronous sequestration of charged organic micro-pollutant onto microwave-assisted hybrid clay materials, Environ. Sci. Pollut. Res., 27 (2020) 9957–9969.
[25] S.E. Agarry, K.M. Oghenejoboh, O.A. Aworanti, A.O. Arinkoola, Biocorrosion inhibition of mild steel in crude oil-water environment using extracts of *Musa paradisiaca* peels, *Moringa oleifera* leaves, and Carica papaya peels as biocidal-green inhibitors: kinetics and adsorption studies, Chem. Eng. Commun., 206 (2019) 98–124.
[26] S. Abbaszadeh, H.R. Nodeh, S.R.W. Alwi, Bio-adsorbent derived from papaya peel waste and magnetic nanoparticles fabricated for lead determination, Pure Appl. Chem., 90 (2018) 79–92.
[27] A. Musa, S.R.W. Alwi, N. Ngadi, S. Abbaszadeh, Effect of activating agents on the adsorption of ammoniacal nitrogen using activated carbon papaya peel, Chem. Eng. Trans., 56 (2017) 841–846.
[28] R. Ahmad, A. Mirza, Heavy metal remediation by dextrin-oxalic acid/cetyltrimethyl ammonium bromide (CTAB) – montmorillonite (MMT) nanocomposite, Groundwater Sustainable Dev., 4 (2017) 57–65.
[29] M. Kumar, R. Tamilarasan, Modeling studies: adsorption of aniline blue by using *Prosopis Juliflora* carbon/Ca/alginate polymer composite beads, Carbohydr. Polym., 92 (2013) 2171–2180.
[30] R. Ahmad, R. Kumar, Adsorptive removal of congo red dye from aqueous solution using bael shell carbon, Appl. Surf. Sci., 257 (2010) 1628–1633.
[31] R.M. Ali, H.A. Hamad, M.M. Hussein, G.F. Malash, Potential of using green adsorbent of heavy metal removal from aqueous solutions: adsorption kinetics, isotherm, thermodynamic, mechanism and economic analysis, Ecol. Eng., 91 (2016) 317–332.
[32] H. Guo, S. Zhang, Z. Kou, S. Zhai, W. Ma, Y. Yang, Removal of cadmium(II) from aqueous solutions by chemically modified maize straw, Carbohydr. Polym., 115 (2015) 177–185.
[33] Q. Wu, R. You, M. Clark, Y. Yu, Pb(II) removal from aqueous solution by a low-cost adsorbent dry desulfurization slag, Appl. Surf. Sci., 314 (2014) 129–137.
[34] I. Hasan, R. Ahamd, A facile synthesis of poly (methyl methacrylate) grafted alginate@Cys-bentonite copolymer hybrid nanocomposite for sequestration of heavy metals, Groundwater Sustainable Dev., 8 (2019) 82–92.
[35] T. Bohli, A. Ouederni, N. Fiol, I. Villaescusa, Evaluation of an activated carbon from olive stones used as an adsorbent for

heavy metal removal from aqueous phases, Comptes Rendus Chimie, 18 (2015) 88–99.
[36] Z. Du, T. Zheng, P. Wang, L. Hao, Y. Wang, Fast microwave-assisted preparation of a low-cost and recyclable carboxyl modified lignocellulose-biomass jute fiber for enhanced heavy metal removal from waterm, Bioresour. Technol., 201 (2016) 41–49.
[37] O.E. Abdel Salam, N.A. Reiad, M.M. ElShafei, A study of the removal characteristics of heavy metals from wastewater by low-cost adsorbents, J. Adv. Res., 2 (2011) 297–303.
[38] R. Ahmad, S. Haseeb, Competitive adsorption of Cu^{2+} and Ni^{2+} on *Luffa acutangula* modified tetraethoxysilane (LAP-TS) from the aqueous solution: thermodynamic and isotherm studies, Groundwater Sustainable Dev., 1 (2015) 146–154.
[39] I. Langmuir, The adsorption of gases on plane surfaces of glass, mica and platinum, J. Am. Chem. Soc., 40 (1918) 1361–1403.
[40] Y. Huang, C. Hsueh, C. Huang, L., Su, C. Chen, Adsorption thermodynamic and kinetic studies of Pb(II) removal from water onto a versatile Al_2O_3-supported iron oxide, Sep. Purif. Technol., 55 (2007) 23–29.
[41] M.J. Temkin, V. Pyzhev, Recent modifications to Langmuir isotherms, Acta Physico-Chimica Sinica, 12 (1940) 217– 225.
[42] S.J. Allen, G. McKay, J.F. Porter, Adsorption isotherm models for basic dye adsorption by peat in single and binary component systems, J. Colloid Interface Sci., 280 (2004) 322–333.
[43] E.A. Dil, M. Ghaedi, A. Asfaram, The performance of nanorods material as adsorbent for removal of azo dyes and heavy metal ions: application of ultrasound wave, optimization and modeling, Ultrason. Sonochem., 34 (2017) 792–802.
[44] R. Ahmad, R. Kumar, S. Haseeb, Adsorption of Cu^{2+} from aqueous solution onto iron oxide coated eggshell powder: evaluation of equilibrium, isotherms, kinetics, and regeneration capacity, Arabian J. Chem., 5 (2012) 353–359.
[45] R. Ahmad, A. Mirza, Sequestration of heavy metal ions by methionine modified bentonite/alginate (Meth-bent/Alg): a bionanocomposite, Groundwater Sustainable Dev., 1 (2015) 50–58.
[46] M. Anbia, Z. Ghassemian, Removal of Cd(II) and Cu(II) from aqueous solutions using mesoporous silicate containing zirconium and iron, Chem. Eng. Res. Des., 89 (2011) 2770–2775.
[47] X. Yang, G. Xu, H. Yu, Removal of lead from aqueous solutions by ferric activated sludge-based adsorbent derived from biological sludge, Arabian J. Chem., 12 (2019) 4142–4149.
[48] A. Mittal, R. Ahmad, I. Hasan, Poly (methyl methacrylate)-grafted alginate/Fe_3O_4 nanocomposite: synthesis and its application for the removal of heavy metal ions, Desal. Water Treat., 57 (2016) 19820–19833.
[49] A. Mirza, R. Ahmad, Novel recyclable (Xanthan gum/montmorillonite) bionanocomposite for the removal of Pb(II) from synthetic and industrial wastewater, Environ. Technol. Innov., 11 (2018) 241–252.
[50] C.W. Oo, M.J. Kassim, A. Pizzi, Characterization and performance of *Rhizophora apiculata* mangrove polyflavonoid tannins in the adsorption of copper(II) and lead(II), Ind. Crops Prod., 30 (2009) 152–161.
[51] T.M. Alslaibi, I. Abustan, M.A. Ahmad, A.A. Foul, Kinetics and equilibrium adsorption of iron(II), lead(II), and copper(II) onto activated carbon prepared from olive stone waste, Desal. Water Treat., 52 (2014) 7887–7897.
[52] M. Mohammadi, A. Ghaemi, M. Torab-Mostaedi, M. Asadollahzadeh, A. Hemmati, Adsorption of cadmium(II) and nickel(II) on dolomite powder, Desal. Water Treat., 53 (2015) 149–157.
[53] R. Ahmad, I. Hasan, L-cystein modified bentonite-cellulose nanocomposite (cellu/cys-bent) for adsorption of Cu^{2+}, Pb^{2+}, and Cd^{2+} ions from aqueous solution, Sep. Sci. Technol., 51 (2016) 381–394.
[54] R. Ahmad, S. Haseeb, Adsorptive removal of Pb^{2+}, Cu^{2+} and Ni^{2+} from the aqueous solution by using groundnut husk modified with Guar Gum (GG): kinetic and thermodynamic studies, Groundwater Sustainable Dev., 1 (2015) 41–49.
[55] S.H. Siddiqui, R. Ahmad, Pistachio shell carbon (PSC) – an agricultural adsorbent for the removal of Pb(II) from aqueous solution, Groundwater Sustainable Dev., 4 (2017) 42–48.